Accepted Manuscript

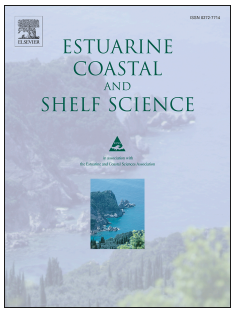

Quartz grains reveal sedimentary palaeoenvironment and past storm events: A case study from eastern Baltic

Edyta Kalińska-Nartiša, Normunds Stivrins, Ieva Grudzinska

PII: S0272-7714(17)30744-8

DOI: 10.1016/j.ecss.2017.11.027

Reference: YECSS 5684

To appear in: *Estuarine, Coastal and Shelf Science*

Received Date: 21 July 2017

Revised Date: 20 November 2017

Accepted Date: 24 November 2017

Please cite this article as: Kalińska-Nartiša, E., Stivrins, N., Grudzinska, I., Quartz grains reveal sedimentary palaeoenvironment and past storm events: A case study from eastern Baltic, *Estuarine, Coastal and Shelf Science* (2017), doi: 10.1016/j.ecss.2017.11.027.

Sediment core of the Lake Lilaste, Latvia

Depth, cm

Age, cal BP

Lithology description

Sediment origin

Types of quartz grains in scanning electron microscope

Diatoms

Depth, cm	Age, cal BP	Lithology description	Sediment origin
	4000	Gyttja, dark brown	
	4400	Gyttja, dark brown	
550	4800	Gyttja, grey	sea
600	5200		
650	5600	Gyttja, brown laminated	storm
700	6000		storm
750	6400		
800	6800	Gyttja, brown	storm
850	7200	Gyttja, dark brown	
900	7600	Gyttja, dry very dark brown	land
950	8000		
1000	8400	Gyttja, black-brown	

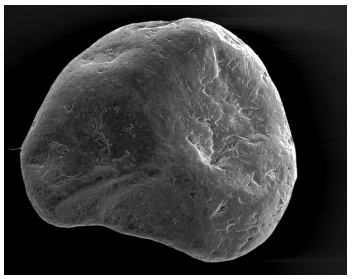

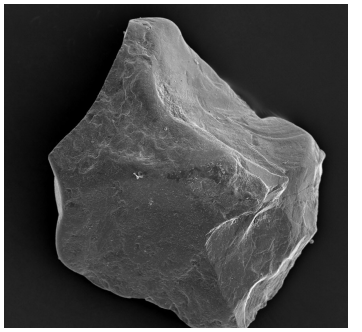

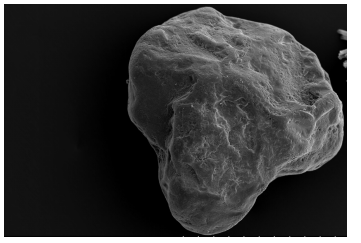

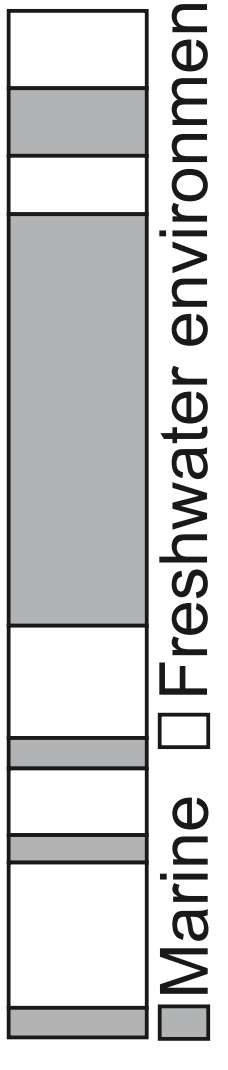

Quartz grains reveal sedimentary palaeoenvironment and past storm events: a case study from eastern Baltic

Edyta Kalińska-Nartiša[1*]; Normunds Stivrins[2,3,4]; Ieva Grudzinska[5,6,7]

[1] University of Tartu, Institute of Ecology and Earth Sciences, Department of Geology, Ravila 14A, EE-50411 Tartu, Estonia; [*] corresponding author: edyta.kalinska-nartisa@ut.ee

[2] Department of Geography, Faculty of Geography and Earth Sciences, University of Latvia, Riga, Jelgavas street 1, LV-1004, Latvia; normunds.stivrins@lu.lv

[3] Department of Geosciences and Geography, University of Helsinki, PO Box 64, FI-00014, Helsinki, Finland

[4] Institute of Geology at Tallinn University of Technology, Ehitajate tee 5, 19086, Tallinn, Estonia

[5] Institute of Plant Sciences, University of Bern, Altenbergrain 21, CH-3013 Bern, Switzerland; ieva.grudzinska@ips.unibe.ch

[6] Oeschger Centre for Climate Change Research, University of Bern, Falkenplatz 16, CH-3013 Bern, Switzerland

[7] University of Latvia, Institute of Biology, Miera iela 3, Salaspils, LV-2169, Latvia; ieva.grudzinska@lu.lv

Abstract

Sediment record collected from the coastal lake serves as a powerful tool for reconstructing changes in palaeoenvironment and understanding the potential signals of past storminess. In this study, we use several proxies from sediment of the Holocene Thermal Maximum at coastal Lake Lilaste, Latvia. We focus on surface texture of quartz grains from the mineral inorganic fraction as indicators of depositional environments. We then use this as a proxy for potential storm transport and combine with information on granulometry, diatom stratigraphy and chronology to answer the question whether flux of quartz grains in the lake originated from the sea or from the land. Analyses in a binocular and scanning electron microscope reveal that most of the investigated quartz grains originate from dwelling in the seawater and wave action in the nearshore zone. Grains representing very energetic subaqueous environment similar to storm events are also present. Terrestrial record is of minor significance and visible through occurrence of aeolian quartz grains.

During drier and colder conditions, an influx of sand with aeolian imprint was delivered to the lake between 8,500 and 7,800 cal yr BP. Marine and terrestrial conditions alternated between 7,800 and 6,000 cal yr BP. Storm-induced grains were likely deposited three times: at 7,300 cal yr BP, 6,600–6,400 cal yr BP, and 6,200–6,000 cal yr BP. Overall stable marine environmental conditions prevailed between 6,000 and 4,000 cal yr BP except of the last portion of terrestrial-induced sediment at 4,100 cal yr BP.

Keywords

palaeostorms, scanning electron microscope, grain size, Holocene Thermal Maximum, Baltic Sea, Gulf of Riga

Highlights

Quartz grain characteristics combined with other proxies as indicators of depositional environments and past storminess

Three palaeostorm events occurred at 7,300 cal yr BP, between 6,600 cal yr BP and 6,400 cal yr BP, and between 6,200 and 6,000 cal yr BP

Marine-terrestrial alternation occurred between 7,800 and 6,000 cal yr BP, and relatively stable marine conditions between 6,000 and 4,000 cal yr BP

1. Introduction

Coastal storms are one of the most dangerous and yet most common threats, and its geological identification enables to predict event re-occurrence (Morton *et al.* 2007) and assess the risk of coastal hazards (Costa *et al.* 2012; McGranahan *et al.* 2007). Recent studies suggest that periods of increased storminess in Northern Europe coincide with changes in atmospheric circulation in the North Atlantic region (de Jong *et al*. 2006; Orme *et al*. 2015). Normally, storminess is defined as a number of days with strong winds in range 7 to 11 on the Beaufort wind scale for one or more measurements during a 6-h period over the course of any single day (Qian and Saunders 2003). Recent and current storminess is relatively easy to estimate from available monitoring data, but it becomes challenging to obtain long-term patterns. In addition, long-term (centuries to millennia)

data could indicate the periods of increased storminess in the past unveiling awareness of extreme weather impact on coastal areas.

The storm surges are high-energy events (Kortekaas and Dawson 2007), thus associated with a complex transport and depositional processes (Costa *et al.* 2012). These events also result in a set of numerous characteristics (Kortekaas 2002; Kortekaas and Dawson 2007). One of them can be recognized as a shallow-sourced marine, beach or coastal dune sediment with a stratigraphically narrow band and a large lateral extension (Costa *et al.* 2012). Consequently, the coastal lakes, lagoons and maritime bogs at the back of coastal barriers provide a relevant geomorphic setting to track palaeostorm activity (Degeai *et al.* 2015; de Jong *et al.* 2006; Dezileau *et al.* 2011; Lane *et al.* 2011; Otvos 2011; Sabatier *et al.* 2010; Tweel and Turner 2012; Van den Biggelaar *et al.* 2014). Sediment records collected in these environments often show coarse-grained layers interbedded with finer-grained, organic-rich autochthonous sediments, where the sand can be interpreted as hurricane-induced event beds (Wallace *et al.* 2014).Variety of proxies allows to distinguish a storm record and this can be done for example through foraminifera (Polovodova Asteman *et al.* 2013; Strotz *et al.* 2016), diatom (Szkornik *et al.* 2008) or pollen analysis (Caseldine *et al.* 2005; Tisdall *et al.* 2013) along with isotopic geochemistry (Das *et al.* 2013; Heyng *et al.* 2012; Sabatier *et al.* 2010). Equally important are studies of internal landform architecture (Vilumaa *et al.* 2016), grain-size (Feal-Perez *et al.* 2014; Klostermann *et al.* 2014; Peros *et al.* 2015; Toomey *et al.* 2013), mineralogy (Klostermann and Gischler 2015) and the character of quartz grains (Björck and Clemmensen 2004; Costa *et al.* 2012; Costas *et al.* 2012).

Bearing in mind future possible climate warming (Vitousek *et al*. 2017), it is crucial to understand patterns of coastal storms and storminess under 2–3º C warmer climate conditions than today. The last time, when such climatic conditions prevailed in Northern Europe was approximately 8,000 to 4,000 years ago during the Holocene Thermal Maximum (=HTM; Heikkilä and Seppä 2010; Renssen *et al*. 2012). Hence, studying sedimentary environment of the HTM affords a relevant insight of future scenario under ongoing climate change.

Here we study storminess patterns during the HTM based on detailed study of coastal Lake Lilaste, Latvia, located near to the Baltic Sea (Fig. 1A, B). Since southeastern coastal sector of the Baltic Sea indicates the same rate of isostatic uplift as the water level increase throughout the HTM (Grudzinska *et al*. 2017), lakes located here have been at the same elevation in comparison to the sea level, that is a crucial aspect when disentangle probable storminess signal from the lake sediment sequence. Lake is situated only one kilometre from the sea, meaning that this lake's sediment is relevant to track past storms and our study has a potential link to these past extreme events. Distinguishing between marine and terrestrial sediment record based on character of quartz

grains is crucial for this study. We use a binocular microscope supplemented by a scanning electron microscope (SEM), which allows direct observation of quartz grains and determining specific sedimentary environment (Krinsley and Takahasi 1962 a, b; Krinsley and Donahue 1968; Krinsley and Doornkamp 1973) such as glacial (Immonen 2013; Immonen *et al.* 2014; Kirshner and Anderson 2011; St. John *et al.* 2015), glaciolacustrine (Mahaney *et al.* 2004), aeolian (Chakroun *et al.* 2009; Kalińska-Nartiša and Nartišs 2016; Kenig 2006; Lisá 2004;), coastal (Armstrong-Altrin and Natalhy-Pineda 2013; Costa *et al.* 2012) and fluvial (Helland and Diffendal 1997; Skolasińska *et al.* 2014). This tool has been not applied to lacustrine deposits in Latvia before, and this archive is fairly undiscovered in this respect. Apart of this, we use a combination of other proxies as diatom stratigraphy and granulometry to improve our understanding about the environmental context of our findings on quartz grains.

2. Location and geological background

Lake Lilaste is located next to the Gulf of Riga, which is a sub-basin of the Baltic Sea. This region is closely related with the atmospheric circulation and cyclonic activity over the North Atlantic (Rutgersson *et al*. 2014). Because currently a significant positive trend for storminess over the whole 20th century exists in Europe (Donat *et al*. 2011), also in the eastern Baltic Sea the maxima of storm surge heights exhibit a substantial increase (Soomere and Pindsoo 2016).

In the historical times (Clarke and Rendell 2009) and geological past (Noren *et al*. 2002), reinforced wind activity associated with a more frequent passage of cyclones took place in Northern Europe (Sorrel *et al*. 2012), and similar record is expected in the Baltic Sea. For example, 1133 storm days were recorded during 57 years of observation in the 20th century in western coast of Estonia (Jaagus *et al.* 2008). The biggest storm surge during the last 2000 years, which took place in 1497, was noted in the Polish coast (Piotrowski *et al.* 2017). Apart of this, tsunami events were caused in the Baltic coast by numerous Holocene earthquakes after the last deglaciation (Mörner 1996, 1999), leaving odd layers in the normal lake deposits with specific pelagic microfossils (Mörner 2008).

Located about 20 km northeast of Riga, at an altitude of 0.5 m a.s.l., Lake Lilaste has a surface of ca. 1.8 km^2 and average water depth of 2.0 m. The entire area is situated within the Valdemārpils glacial phase, which is the latest deglaciation stage of the Scandinavian Ice Sheet in Latvia, and its limit stretches along the modern sea-coast in this part of Latvia (Zelčs *et al*. 2011). Devonian sandstone and clay (30–40 m b.s.l.) form the bedrock, overlain by ca. 45 m thick Weichselian till and glaciolacustrine and marine silt, sand and aeolian deposits.

3. Material and methods

We studied sediment core from Lake Lilaste, which has been sampled in 2013 through the ice and studied by means of diatom, loss-on-ignition and magnetic susceptibility analyses (Grudzinska *et al*. 2017). Importantly, the Lake Lilaste sediment sequence owes the well-established chronology based on AMS and conventional radiocarbon dates (Grudzinska *et al*. 2017). Current study focuses at the sediments granulometry and surface texture of quartz grains from the mineral fraction.

3.1. Granulometry

The grain size distribution was studied for continuous 2-cm thick samples from the depth 500–1028 cm that covers time span from 3,960 to 8,440 cal BP. The sediment samples were prepared by using the HCl + H_2O_2 method described in Vaasma (2008). At first, the sediment samples were treated by 10% HCl solution to dissolve carbonates, metal salts, and oxides. After the sediments were washed by distilled water and centrifuged, 30% H_2O_2 was added to remove the organic matter. When the active reaction ended, to achieve a neutral environment the samples were washed with distilled water, centrifuged and decanted three times. Particle size distribution analyzer "Partica" LA-950V2 was used to determine granulometry of the sediments. The results of grain size distribution are represented as a percentage in each particle class: clay (<0.002 mm), fine silt (0.002–0.0063 mm), medium silt (0.0063–0.02 mm), coarse silt (0.02–0.063 mm), fine sand (0.063–0.2 mm), medium sand (0.2–0.63 mm) and coarse sand (0.63–2 mm) following the Udden-Wentworth grain-size scale (Wentworth 1922). The grain size statistics were calculated using Gradistat v. 8 (Blott and Pye 2001). Finally, biplots of mean versus sorting and sorting versus skewness were constructed following recommendation of Martins (2003) modified after Friedman (1967).

3.2. Analysis in a binocular microscope

The 0.1–0.2 mm sand fraction from 138 samples (2-cm thick) was used to determine grain rounding and character of surface under a binocular microscope with ca. 50× magnification. Wet sieving was performed prior to the analysis to obtain this fraction. Quartz grains were summarised as (1) grain shape: angular – partially rounded – well rounded, and (2) surface type: matte – shiny following the Cailleux (1942) methodology extended by Mycielska-Dowgiałło and Woronko (1998). Whereas roundness largely depends on the residence time in a given environment, the surface character reflect the nature of the environment (Woronko and Pisarska-Jamroży 2016). Following this statement, quartz grains were classified to one of the six groups: (1) aeolian, well-

rounded and matte across the whole surface (RM), (2) aeolian, partially rounded and matte only on the most convex part of the grain (EM/RM), (3) high energetic subaqueous environment, well rounded and shiny (EL), (4) high energetic subaqueous environment, partially rounded and shiny (EM/EL), (5) with fresh surfaces and edges, without chemical weathering and transportation impact (NU), and (6) cracked with at least 30% of the original grain surface (C).

3.3. Analysis in a scanning electron microscope

A total of 80 quartz grains corresponding to 5 sediment samples were selected and prepare for analyses with SEM. Prior to the analyses quartz grains were placed on SEM stub with a help of binocular microscope and sputter-gold coated in order to generate sharper images and reduce electrical charging of the surface (Vos *et al.* 2014). Quartz grains were imaged with ca. 100-times to determine their roundness (rounded, subangular, angular), and ca. 400–1200-times to determine presence of mechanical, chemical and combined microtextures on their surface. To facilitate identification and comparative analysis of different microtextures, an atlas based upon the work of Mahaney (2002) and a semi-quantitative approach to the microtextural classification of each grain, based upon the proportion of grain surface occupied by each feature as proposed by Vos *et al.* (2014) with a slight modifications were used. Additionally, mechanically induced microtextures were grouped in three genetic classes (1) high-stress fractures, (2) percussion, and (3) polygenetic fractures as proposed by Sweet and Soreghan (2010).

3.4. Principal Component Analysis

Principal Components Analysis (PCA) was performed to estimate the variability among samples and to see the major trends between environmental proxies. As the data were compositional and had a gradient 1.0 standard deviation (SD) units long, linear ordination method namely PCA was used with log transformation of data prior analysis. CANOCO 5.04 (ter Braak and Šmilauer 2012) was used for PCA. In PCA we included: 1) relative abundance of main diatom groups indicating freshwater, marine-brackish and turbid water environment obtained from Grudzinska *et al*. (2017); 2) mineral matter indicating relative abundance of inorganic content in the sediment (Grudzinska *et al*. 2017); 3) data of minerogenic grain fraction size (silt, clay and sand) relative abundance in gyttja; 4) relative abundance of specific quartz grain morphological features, such as roundness and surface shininess suggesting grain transportation pathways (e.g. Kalińska-Nartiša *et al*. 2017a, b).

To avoid collinearity, we left out strongly correlated variables prior to the analysis, i.e. content of organic matter, as it was directly inverse to the content of mineral matter.

3.5. Unconstrained cluster analysis

Compositional sample similarities of granulometry and quartz grain morphological features throughout the studied time were characterized by applying a stratigraphically unconstrained cluster analysis – the method of incremental sum-of-squares. Analysis was performed in TILIA 1.7.16. with the CONISS program (Grimm 1987). Unconstrained cluster analysis is independent of time and depth, and clusters are comprised of samples with similar sediment assemblages that are not necessarily adjacent (Grimm *et al*. 2011). In this way, any sample or cluster can merge with any other similar sample or cluster. Hence, each cluster is characteristic with some specific features that allows to discuss similarities within a chosen time period.

4. Results

4.1. Lithology and granulometry

Sediment sequence contains gyttja with variable mineral matter content, where dominant grain size fractions are silt and fine sand (Fig. 2). Distinct mineral matter (42–82 %) fluctuations at 522–980 cm depth indicate constantly changing sedimentation environment from 8,700 cal BP to ca 4,270 cal BP. In addition, sand layers at 595–800 cm depth (5,000–6,700 cal BP) and visually distinct layer with sharp boundary and gradual colour change at 522–540 cm depth (4,270–4,520 cal BP) were observed. In the upper part (500–522 cm) mineral matter content gradually decreases from 78% to 63%. The lithology of Lake Lilaste sediment sequence is described in detail in Grudzinska *et al*. (2017).

The mean grain size (M) varies between 3.4 and 7.1 phi (Fig. 2). The largest proportion of the sediments consists of medium and coarse silt, and fine sand (Fig. 2). A significant amount of medium and coarse sand was deposited at 8,500–7,800 cal BP. Some distinct peaks of medium and coarse sand are also observed at 540–830 cm depth that covers time period between 6,900 and 4,500 cal BP. All investigated sediments are either poorly sorted or very poorly sorted (σ = 1.1-3.3), and negatively to positively skewed (Sk = -0.4-0.4; Fig. 2). In both bivariate plots, all samples

situate out of the river-beach-dune sectors towards higher values of standard deviation and mean (Fig. 3A, B).

4.2. General grain shape and surface character

Quartz grains with shiny surface are the main mineral constituents in the investigated samples. Shiny and partially rounded grains (EM/EL) vary generally between 53% and 96%. Shiny grains with a well-rounded outline (EL) reveal a great variability and differ from 4% to 47%. Content of partially rounded grains with matte surface (EM/RM) is as high as 14%. Occasionally, 21%–42% of these matte grains occur in few sediment horizons. Similarly, grains with fresh surfaces (NU) constitute up to 12% of total number of grains in few sediment horizons.

4.3. Microtextures

SEM analysis reveals quartz grains with two types of outline: subrounded (sometimes with conchoidal features of different size) (Fig. 4a), and rounded angular grains are either absent, or vary only between 5% and 15% in the investigated sediments. The mechanical-origin features on the surface of these grains are moderate or sparse (Fig. 5), but relatively fresh (i.e. Fig. 4A). The rest of investigated samples reveals mechanical microtextures, which are mostly not fresh anymore, and are overprinted by chemical processes (Fig. 4D-E). Among mechanical textures, bulbous edges (Fig. 4B-C) are abundant and V-shaped percussion cracks (Fig. 4F) range from moderate to abundant in the all investigated samples (40-90%; Fig. 5). These cracks are often coupled with crescentic marks (Fig. 4G), which sometimes are widen by solution processes (Fig. 4J). Chemically-induced microtextures seem dominate over these of mechanical origin; solution pits and crevasses are abundant and 85–100% grain surface is intensively precipitated (Figs. 4I–J). Occasionally, precipitation occurs only in depressions (Fig. 4K). Oriented etch pits (Fig. 4L) reveal wide range and vary from 0% to 93%. Most grains exhibit low and medium relief. In contrast, high grain relief is either sparse or absent.

Nearly 100% of all the grains have adhering particles that appear to result from release during grain fracture. A general trend, where the percussion fractures followed by polygenetic group, is observed in all investigated samples. The high-stress microtextures occur on 4 to 15% grain surfaces.

4.4. Principal Components and Cluster Analysis

There are two distinct environmental gradient directions in PCA (Fig. 6). Freshwater environment is characterized by close relationship with sand and marine/brackish environment with mineral matter, silt and clay fractions.

Although no clear connection of quartz grain features to any environment can be draw from PCA, the unconstrained cluster analysis (UCA) reveals additional insights. Altogether six cluster divisions were made based on proxy data sample similarities (Table 1; Fig. 8). If to arrange samples from clusters according their stratigraphical position, similarities and transitions in environmental conditions within the HTM can be observed which are described in Table 1 and illustrated in Figure 8.

5. Discussion

Sediments within back barrier lagoons, as represented by Lake Lilaste, are normally muddy and organic, and occurrence of sand fraction might be interpreted as evidence of storm events (Nott 2014). Our results of granulometry shows that coarser and finer fractions alternate in the investigated sediments, and therefore, allow a preliminary assumption that some sandier horizons are due to storm surges. We discuss this possibility in the following sections.

5.1. Marine or terrestrial signal in quartz grains?

Our study shows that quartz grains with shiny surfaces and with a general rounded (EL) and partially rounded shape (EM/EL) dominate in most investigated samples of Lake Lilaste (Fig. 7). These grains are directly linked with intense abrasive processes, and thus likely originate from marginal marine environments (Madhavaraju *et al.* 2006; Mahaney 2002; Makvandi *et al.* 2015; Moral Cardona *et al.* 1997; Vos *et al.* 2014). This gives us the first assumption that quartz grains found in the lake were largely sourced from the sea. However, terrestrial origin is also somehow present (*see* below).

At least five microtextural features should be taken into account to determine sedimentary environment (Costa *et al.* 2012). Following this recommendation, we consider the most abundant features as (1) grain shape, (2) a general presence of percussion marks and fresh surfaces (=conchoidal features), (3) V-shaped percussion cracks, (4) oriented etch pits, and (5) precipitation,

are the most important features to help to explain the evidence for either marine or terrestrial grain source.

The overall grain shape, as seen under SEM (Figs. 4, 5), is similar with results from the binocular microscope; subrounded and rounded grains again prevail and the percussion marks such as V-shaped cracks occur on their surface. The origin of V-shaped cracks has been a matter of debate (cf. Costa *et al.* 2012), however, these cracks are surely linked with grain-to-grain collision, typically associated with high-energy, subaqueous conditions such as wave action in the nearshore zone (Culver *et al.* 1983; Mahaney and Kalm 2000). Increasing frequency of V-shaped cracks is produced even in short-period event in exceedingly high wave velocity during tsunami (Mahaney and Dohm 2011). In this study, moderate and abundant occurrence of V-shaped cracks, thus lesser grain damage indicate a lower-energy impact than triggered during the large tsunamis.

A great nearshore influence is further seen as defects in the crystal lattice (Vos *et al.* 2014). Dwelling in the seawater (Bull 1981), nearshore (Gutiérrez-Mas *et al.* 2003) or arid coastal environment (Newell *et al.* 2015) can result in presence of the oriented pitting in grain surface, and this means, that most of the investigated quartz grains were in contact with alkaline fluids such as seawater.

Chemical action results also in mineral precipitation and adherence of minute particles (Warrier *et al.* 2015), which are relevant in the investigated grains. However, continuous wave movement should have washed out all adhering particles (Costa *et al*. 2009). In this study, a high number of dissolution and adhering particles may be due to percolating water flow, rather than active wave movement, as also observed by Bellanova et al. (2016). Limited active wave movement is also probably a cause of not fresh percussion marks.

Storm quartz grains are, in contrast, characterized by more percussion marks and fresh surfaces compared to potential source material (Bruzzi and Prone 2010; Costa *et al*. 2017), suggesting derivation from offshore areas not subjected to beach rounding (Dahanayake and Kulasena 2008). Therefore, cracked grains with numerous fresh big-sized conchoidal features (Fig. 4B), for example as observed in the sediment deposited at 5,900 cal BP, and fresh grains (NU; Fig. 4A) visible in a few sediment horizons, suggest a storm record. Great grain damage results from a very energetic subaqueous environment with shallow seafloors (Gutiérrez-Mas *et al.* 2003; Kalińska-Nartiša *et al.*, 2017a), where the breaking of waves is dominant transport agent (Costa *et al*. 2012).

In contrast, terrestrial signal is minor in this study, and represented only in few parts of investigated profile. Here, partially or quartz grains with matte surface occur, which clearly suggests subaerial environment with predominance of aeolian factor (Mycielska-Dowgiałło and Woronko 2004; Refaat and Hamdan 2015; Vos *et al*. 2014). Considering that aeolian grains dominate in some

surficial sediments in the region (Kalińska-Nartiša *et al*. 2016), these grains were likely blown away as airborne material.

5.2. Likely storminess versus aeolian activity

A general distinction of storm surge versus aeolian sourced material may be difficult. Therefore, a support by, for example, biogenic material of marine origin, is strongly recommended (Hippensteel *et al*. 2008). Studies on biogenic material are relevant in this study, and the UCA (*see* Results and Figs. 6, 7) greatly helps to distinguish between storm and aeolian record. Applying this method, we know that in the third, fourth, fifth and sixth zones marine conditions prevailed as revealed by the main marine and brackish diatom groups. However, quartz grains features indicate that only the third and fourth zone likely represent marine and storm signals, respectively, because agreement between record of biogenic and mineral material exists as should be normally considered according to Hippensteel *et al*. (2008). In other words, both marine diatom species and marine signal in quartz grains coincide in the third and the fourth zone. The fifth and sixth zones carry, in contrast, rather an aeolian record, along with the first and the second zones, which further coincide with abundance of freshwater diatom species (Fig. 7).

The bottommost part of the investigated profile with age between 8,500 and 7,800 cal yr BP reveals features of the second zone. A closer look into this zone shows only limited aeolian signal (=few aeolian-type grains) with a simultaneous increase in fine-, medium- and coarse-sand fractions (Fig. 2) together with a higher than elsewhere in the profile value of magnetic susceptibility (Grudzinska et al. 2017). At this time frame, an influx of sand with minor aeolian imprint and presumably heavy mineral fraction was delivered to the lake. This was due to aeolian activity, which was triggered by drier (Hammarlund *et al.* 2003) and colder (Veski *et al*. 2004) conditions in the region, which also resulted in accumulation of the inland aeolian landforms in Latvia (Kalińska-Nartiša *et al*. 2016; Nartišs and Kalińska-Nartiša 2017). Nevertheless, an unusual thin sand layer within the peat bed, which accumulated before 8,400–8,200 cal yr BP, was found in the neighbouring southwestern Estonian coast, and correlated either with storm surges or tsunami-type sedimentation (Veski *et al.* 2005). The latter scenario could have been generated either by the Storegga slide, which left deposits in coastal areas around the Norwegian Sea and North Sea (Bondevik *et al.* 1998, 2005), or alternatively, by a meteorite impact event, which has been recorded as a layer of siliceous microshperules in peat bogs in the West Estonian Archipelago at this time frame (Raukas 2000). However, no similar record has been studied or found in the Lilaste Lake.

Our proxy certainly allows to state that environmental conditions intensively alternated from marine to terrestrial between 7,800 and 6,000 cal yr BP. At this time span, we have presumably detected three storm events. Along with the previous diatom study (Grudzinska *et al*. 2017), seawater surges occurred in Lake Lilaste at 7,600 and 7,300 cal yr BP. However, we have not observed a similar storm signal from the grain proxy at 7,600 cal yr BP. This is likely because a clay fraction (*see* the fifth zone in Fig. 8), resulting in higher content of the mineral matter, but not sand fraction was delivered to the lake. Since clay material may have deposited in progressively lower energy conditions favoured by the presence of the barrier (Quintela *et al*. 2016), this fact diminished a role of strong surges at 7,600 cal yr BP. Conversely, a presence of larger grains with fresh surfaces and conchoidal features at ca. 7,300 cal yr BP, as apparent from the fourth zone and SEM analysis, suggests more predominant storminess (Stanley and Deckker 2002) and the first storm signal recorded in the investigated profile. SEM grain proxy shows similar trend also at 7,200 cal yr BP (sample LI 860 cm, Fig. 5), though the UCA correlates rather with the third (=marine) zone than with the fourth (=likely storm) zone (Fig. 8).

Further potential palaeostorm signals are related with a long-term, intermittent inputs of sea water observed between 6,700 and 4,200 cal yr BP (Grudzinska *et al*. 2017). Also, our quartz grain proxy supports this, since mostly continuous delivery of sediment of marine origin took place at this time. Sediments with storm-induced grains were likely deposited twice in Lilaste: between 6,600 and 6,400 cal yr BP, followed by a 6,200 and 6,000 cal yr BP event, which is additionally supported by SEM findings in sediments of 5,900 cal BP. Influx of sand material (= second zone) occurred at ca. 6,300 cal BP. This marine-terrestrial alternation supports a general statement that atmospheric circulation might have been inconsistent as observed in Europe at this time (Mauri *et al*. 2014). Assuming storm surges in the Gulf of Riga occurred at these times, they may have been responsible for the major re-blowing event of coastal foredunes, which occurred, for example, at 6.3±0.5 ka cal yr BP at Ruhnu Island, 100 km northwest of Lake Lilaste (Muru 2017; Preusser *et al*. 2014). High-energy event layers, but likely representing tsunamis, are known from the Polish coast and their deposition took place between 6,600 and 6,300 cal. yr BP (Rotnicki *et al.* 2016). Similar period of increased storm activity was recorded in the southern Europe (Costas *et al*., 2012; Sabatier *et al*. 2012). However, storm events in the Gulf of Riga occurred earlier than these, observed in the western Swedish coast between 5,700 and 5,450 cal yr BP (Björk and Clemmensen 2004).

A nearly 2 ka period of a relatively stable marine environmental conditions appears from quartz grain proxy and was recorded between 6,000 and 4,000 cal yr BP at Lilaste. At this time, mostly marine transgression took place except of two shorter freshwater events (Grudzinska *et al*. 2017),

and sediments caring marine-induced grains occurred in the investigated profile. Colder (Seppä *et al*. 2009), and likely stormier conditions has been recorded in Europe during termination of the HTM (Björk and Clemmensen 2004; Clemmensen *et al*. 2009, 2012; Costas *et al*. 2012; de Jong *et al*. 2006; Hede *et al*. 2015; Nielsen *et al*. 2016; Sorrel *et al*. 2012). In the neighbouring Lithuanian coastal zone, evidences for a salt water invasion, possibly caused by the tsunami waves, have been found at this time (Bitinas *et al.* 2016; Damušytė 2016). However, we did not detect a similar trend at Lilaste, likely because this site is not directly open to stronger storm surges from the west as in Lithuanian coast. Nevertheless, among single horizons of medium and coarse sand combined with marine features of the third zone no storm-like grains have been found.

As revealed by our study, the last portion of terrestrial-induced sediment occurred in Lake Lilaste at 4,100 cal yr BP, when the lake isolated and brackish-water intrusion was no longer observed (Grudzinska *et al*. 2017).

5.3. Quartz grains as a potential past storminess indicator

Quartz grains found in the sediment of coastal lakes are generally considered as a powerful proxy for palaeoenvironmental reconstructions and palaeostorminess tracking. Nevertheless, some studies are less optimistic and shows that identifying modern hazardous events in the sediments through microtextural analysis may be hampered (Bellanova *et al.* 2016). Based on our study, two aspects must be highlighted. Firstly, we certainly know that not all sand interbeddings, as found in the coastal lake sediments, are related to the storm events. Secondly, only utilizing quartz grain rounding, character of their surface and microtextures on the top of this surface combined with additional proxies can significantly help in distinguishing between marine and terrestrial sediment influx, and indicate past storm events. Certainly, future work at probably higher resolution is still required.

6. Conclusions

Sediment profile of coastal Lake Lilaste, Latvia, located near to the Baltic Sea, allows a better understanding of potential palaeostorm events during the HTM and distinguishing between marine and terrestrial record. To obtain this, we combine multi-proxy sediment analyses as character of quartz grains, diatom stratigraphy, mineral matter content, granulometry and chronology, and test them towards the unconstrained cluster analysis.

Along with the appearance of quartz grains, mineral material found in Lilaste is largely sourced from the sea. This is supported by occurrence of microtextures that originate from dwelling in the seawater and wave action in the nearshore zone. Since surface of some grains is fresh with numerous conchoidal features, these grains indicate the storm events. Terrestrial signal is minor and, in contrast, related to partially or well rounded quartz grains with matte surface. These grains suggest predominance of aeolian conditions.

Such assumptions combined with results of clustering, allow us to distinguish six alternating clusters (zones), which reveal variability of sediment influx in the lake. Between 8,500 cal BP and 7,800 cal BP, during colder and drier regional conditions, fresh sand with minor aeolian imprint on its quartz grains was deposited in the lake. Intense alternation between marine and terrestrial environmental conditions took place between 7,800 and 6,000 cal yr BP. At this period, grain proxy revealed presumably three storm events: at 7,300 cal BP, 6,600–6,400 cal yr BP, and 6,200–6,000 cal BP. Stable marine conditions dominated between 6,000 and 4,000 cal yr BP, except of the portion of terrestrial-induced sediment, which occurred in Lake Lilaste at 4,100 cal yr BP.

Acknowledgements

The study was supported by ESF Grant 9031, IUT 1-8 and the Doctoral Studies and Internationalisation Programme DoRa (to I. Grudzinska), EBOR project and National basic funding for science project Y5-AZ03-ZF-N-110 “Dabas resursu ilgtspējīga izmantošana klimata pārmaiņu kontekstā” Nr. ZD2010/AZ03 (to N. Stivrins), the SIA SunGIS and by the Mobilitas Pluss project MOBTP34 “Time-transport-storminess – an experimental geological study of coastal system” (to E. Kalińska-Nartiša). Our manuscript has been improved by the comments of three anonymous reviewers.

References

Armstrong-Altrin, J.S., Natalhy-Pineda, O., 2013. Microtextures of detrital sand grains from the Tecolutla, Nautla, and Veracruz beaches, western Gulf of Mexico, Mexico: implications for depositional environment and paleoclimate. Arab. J. Geosci. 7, 4321–4333. doi:10.1007/s12517-013-1088-x

Bellanova, P., Bahlburg, H., Nentwig, V., Spiske, M., 2016. Microtextural analysis of quartz grains of tsunami and non-tsunami deposits – A case study from Tirúa (Chile). Sediment. Geol. 343, 72–84. doi:10.1016/j.sedgeo.2016.08.001

Bitinas, A., Damušytė, A., Vaikutienė, G., 2016. Post-glacial seismic activity on the south-eastern coast of the Baltic Sea, in: Kramarska, R., Pączek, U. Uścinowicz, G., Uścinowicz, Sz., Woźniak,

M. (Eds.), Abstract volume and field trip guidebook. The 13th Colloquium on Baltic Sea Marine Geology, 12-16.09.2016, Gdańsk, Poland, pp. 47.

Björk, S., Clemmensen, L.B., 2004. Aeolian sediment in raised bog deposits, Halland, SW Sweden: a new proxy record of Holocene winter storminess variation in southern Scandinavia? The Holocene 14(5), 677-688. doi: 10.1038/nclimate2923

Blott, S.J., Pye, K., 2001. Gradistat: a grain size distribution and statistic package for the analysis of unconsolidated sediments. Earth Surf. Proc. Land. 26, 1237–1248. doi:10.1002/esp.261

Bondevik, S., Svendsen, J.I, Mangerud, J., 1998. Distinction betweem the Storegga tsunami and the Holocene marine transgresion in coastal deposits of western Norway. J. Quat. Sci. 13(6), 529–537. doi:10.1002/(SICI)1099-1417(1998110)13:6<529::AID-JQS388>3.0.CO;2-1

Bondevik, S., Løvholt, F., Harbitz, C., Mangerud, J., Dawson, A., Svendsen, J.I., 2005. The Storegga Slide tsunami–comparing field observations with numerical simulations. Mar. Petr. Geol. 22, 195–208. doi:10.1016/j.marpetgeo.2004.10.003

Bruzzi, C., Prone, A., 2000, A method of sedimentological identification of storm and tsunami deposits: exoscopic analysis, preliminary results. Quat. 11(3-4), 167–177. doi:10.3406/quate.2000.1666

Bull, P.A., 1981. Environmental reconstruction by electron microscopy. Prog. Phys. Geogr. 5, 368–397.

Cailleux, A., 1942. Les actiones éoliennes périglaciaires en Europe. Mémoires la Société Géologique Fr. 41, 1–176.

Caseldine, C., Thompson, G., Langdon, C., Hendon, D., 2005. Evidence for an extreme climatic event on Achill Island, Co. Mayo, Ireland around 5200-5100 cal. yr BP. J. Quat. Sci. 20, 169–178. doi:10.1002/jqs.901

Chakroun, A., Miskovsky, J.-C., Zaghbib-Turki, D., 2009. Quartz grain surface features in environmental determination of aeolian Quaternary deposits in northeastern Tunisia. Mineral. Mag. 73, 607–614. doi:10.1180/minmag.2009.073.4.607

Clarke, M.L., Rendell, H.M., 2009. The impact of North Atlantic storminess on western European coasts: A review. Quat. Int. 195, 31–41. doi:10.1016/j.quaint.2008.02.007

Clemmensen, L.B., Murray, A., Heinemeier, J., de Jong, R., 2009. The evolution of Holocene coastal dunefields, Jutland, Denmark: A record of climate change over the past 5000 years. Geomorphology 105, 303–313. doi:10.1016/j.geomorph.2008.10.003

Clemmensen, L.B., Murray, A.S., Nielsen, L., 2012. Quantitative constraints on the sea-level fall that terminated the Littorina Sea Stage, southern Scandinavia. Quat. Sci. Rev. 40, 54–63. doi:10.1016/j.quascirev.2012.03.001

Costa, C.S.B., Iribarne, O., Farina, J.M., 2009. Human impacts and threats to the conservation of South American salt marshes, in: Silliman, B.R., Grosholtz, E.D., Bertness, M.D. (Eds.), Human Impact on Salt Marshes. A Global Perspective. University of California Press, pp. 337–360.

Costa, P.J.M., Andrade, C., Freitas, M., Oliveira, M., Lopes, V., Dawson, A., Moreno, J., Fatela, F., Jouanneau, J.-M., 2012. A tsunami record in the sedimentary archive of the central Algarve coast, Portugal: Characterizing sediment, reconstructing sources and inundation paths. The Holocene 22, 899–914. doi:10.1177/0959683611434227

Costa, P.J.M., Gelfenbaum, G., Dawson, S., Selle, S. La, Milne, F., Cascalho, J., Lira, C.P., Andrade, C., Freitas, M.C., Jaffe, B., 2017. The application of microtextural and heavy mineral analysis to discriminate between storm and tsunami deposits. Geol. Soc. London, Spec. Publ. 456. doi:10.1144/SP456.7

Costas, S., Jerez, S., Trigo, R.M., Goble, R., Rebêlo, L., 2012. Sand invasion along the Portuguese coast forced by westerly shifts during cold climate events. Quat. Sci. Rev. 42, 15–28. doi:10.1016/j.quascirev.2012.03.008

Culver, S.J., Bull, P.A., Campbell, S., R.A., S., Whalley, W.B., 1983. Environmental discrimination based on quartz grain surface textures: a statistical investigation. Sedimentology 30, 129–136.

Dahanayake, K., Kulasena, N., 2998. Recognition of diagnostic criteria for recent- and paleo-tsunami sediments from Sri Lanka. Mar. Geol. 254, 180–186. doi:10.1016/j.margeo.2008.06.005

Damušytė, A., 2016. Possible paleo-tsunamis footprints in the Baltic Sea south-eastern coast, in: IGCP Project 639 “Sea Level Change from Minutes to Millennia”. First project meeting 9-14 November 2016, Muscat, Oman, pp. 33–34.

Das, O., Wang, Y., Donoghue, J., Xu, X., Coor, J., Elsner, J., Xu, Y., 2013. Reconstruction of paleostorms and paleoenvironment using geochemical proxies archived in the sediments of two coastal lakes in northwest Florida. Quat. Sci. Rev. 68, 142–153. doi:10.1016/j.quascirev.2013.02.014

Degeai, J.P., Devillers, B., Dezileau, L., Oueslati, H., Bony, G., 2015. Major storm periods and climate forcing in the Western Mediterranean during the Late Holocene. Quat. Sci. Rev. 129, 37–56. doi:10.1016/j.quascirev.2015.10.009

de Jong, R., Björck, S., Björkman, L., Clemmensen, L.B., 2006. Storminess variation during the last 6500 years as reconstructed from an ombrotrophic peat bog in Halland, southwest Sweden. J. Quat. Sci. 21, 905–919. doi:10.1002/jqs.1011

Dezileau, L., Sabatier, P., Blanchemanche, P., Joly, B., Swingedouw, D., Cassou, C., Castaings, J., Martinez, P., Von Grafenstein, U., 2011. Intense storm activity during the Little Ice Age on the French Mediterranean coast. Palaeogeogr. Palaeoclimatol. Palaeoecol. 299, 289–297. doi:10.1016/j.palaeo.2010.11.009

Donat, M.G., Renggli, D., Wild, S., Alexander, L. V., Leckebusch, G.C., Ulbrich, U., 2011. Reanalysis suggests long-term upward trends in European storminess since 1871. Geophys. Res. Lett. 38, 1–6. doi:10.1029/2011GL047995

Ekman, M., 1996. A consistent map of the postglacial uplift of Fennoscandia. Terra Nova 8, 158-165.

Feal-Perez, A., Blanco-Chao, R., Ferro-Vazquez, C., Martinez-Cortizas, A., Costa-Casais, M., 2014. Late-Holocene storm imprint in a coastal sedimentary sequence (Northwest Iberian coast). The Holocene 24, 477–488. doi:10.1177/0959683613520257

Friedman, G., 1967. Dynamic processes and statistical parameters compared for size frequency distributions of beach and river sands. J. Sed. Petr. 37(2). 327–364.

Grimm, E.C., 1987. CONISS: a FORTRAN 77 program for stratigraphically constrained cluster analysis by the method of incremental sum of squares. Comput. Geosci. 13, 13–35.

Grimm, E.C., Donovan, J.J., Brown, K.J., 2011. A high-resolution record of climate variability and landscape response from Kettle Lake, northern Great Plains, North America. Quat. Sci. Rev. 30, 2626–2650. doi:10.1016/j.quascirev.2011.05.015

Grudzinska, I., Vassiljev, J., Saarse, L., Reitalu, T., Veski, S., 2017. Past environmental change and seawater intrusion into coastal Lake Lilaste, Latvia. J. Paleolimnol. 57, 257–271. doi:10.1007/s10933-017-9945-3

Gutiérrez-Mas, J.M., Moral, J.P., Sánchez, a., Dominguez, S., Muñoz-Perez, J.J., 2003. Multicycle sediments on the continental shelf of Cadiz (SW Spain). Estuar. Coast. Shelf Sci. 57, 667–677. doi:10.1016/S0272-7714(02)00407-9

Hammarlund, D., Björk, S., Buchardt, B., Israelson, C., Thomsen C.T., 2003. Rapid hydrological changes during the Holocene revealed by stable isotope record of lacustrine carbonates from Lake Igelsjön, southern Sweden. Quat. Sci. Rev. 22, 353–370. doi:10.1016/S0277-3791(02)00091-4

Hede, M.U., Sander, L., Clemmensen, L.B., Kroon, A., Pejrup, M., Nielsen, L., 2015. Changes in Holocene relative sea-level and coastal morphology: A study of a raised beach ridge system on Samso, southwest Scandinavia. The Hol. 25, 1402–1414. doi:10.1177/0959683615585834

Heikkilä, M., Seppä, H., 2010. Holocene climate dynamics in Latvia, eastern Baltic region: a pollen-based summer temperature reconstruction and regional comparison. Boreas 39, 705–719. doi:10.1111/j.1502-3885.2010.00164.x

Helland, P.E., Diffendal, R.F., 1997. SEM analysis of quartz sand grain surface textures indicates alluvial/colluvial origin of the Quaternary “Glacial” Boulder Clays at Huangshan (Yellow Mountain), East-Central China. Quat. Res. 48, 177–186. doi:10.1006/qres.1997.1916

Heyng, A.M., Mayr, C., Lücke, A., Striewski, B., Wastegård, S., Wissel, H., 2012. Environmental changes in northern New Zealand since the Middle Holocene inferred from stable isotope records (δ15N, δ13C) of Lake Pupuke. J. Paleolimnol. 48, 351–366. doi:10.1007/s10933-012-9606-5

Hippensteel, S.P., Eastin, M.D., Garcia, W.J., Sciences, E., 2008. The geological legacy of Hurricane Irene: Implications for the fidelity of the paleo-storm record. GSA Today 23, 4–10. doi:10.1130/GSATG184A.1

Immonen, N., 2013. Surface microtextures of ice-rafted quartz grains revealing glacial ice in the Cenozoic Arctic. Palaeogeogr. Palaeoclimatol. Palaeoecol. 374, 293–302. doi:10.1016/j.palaeo.2013.02.003

Immonen, N., Strand, K., Huusko, A., Lunkka, J.P., 2014. Imprint of late Pleistocene continental processes visible in ice-rafted grains from the central Arctic Ocean. Quat. Sci. Rev. 92, 133–139. doi:10.1016/j.quascirev.2014.01.008

Jaagus, J., Post, P., Tomingas, O., 2008. Changes in storminess on the western coast of Estonian in relation to large-scale atmospheric circulation. Clim. Res. 36, 29-40. doi: 10.3354/cr00725

Kalińska-Nartiša, E., Nartišs, M., 2016. Sandy fan-like forms in the central-eastern Mazovian Lowland (Central Poland): textural record and chronology. Geogr. Ann. Ser. A. Phys. Geogr. 98, 111–127. doi:10.1111/geoa.12125

Kalińska-Nartiša, E., Thiel, C., Nartišs, M., Buylaert, J-P., Murray, A.S., 2016. The north-eastern aeolian “European Sand Belt” as potential record of environmental changes: A case study from Eastern Latvia and Southern Estonia. Aeol. Res. 22, 59-72. doi:10.1016/j.aeolia.2016.06.002

Kalińska-Nartiša, E., Alexanderson, H., Nartišs, M., Stevic, M., Kaiser, K., 2017a. Sedimentary features and transportation pathways of the Holocene and Lateglacial sediments in the Kristianstad plain, SE Sweden. Gff 139, 147–161

Kalińska-Nartiša, E., Woronko, B., Ning, W., 2017b. Microtextural inheritance on quartz sand grains from Pleistocene periglacial environments of the Mazovian Lowland, central Poland. Permafr. Periglac. Process. 28(4), 741-756. doi:10.1002/ppp.1943

Kenig, K., 2006. Surface microtextures of quartz grains from Vistulian loesses from selected profiles of Poland and some other countries. Quat. Int. 152–153, 118–135. doi:10.1016/j.quaint.2005.12.015

Kirshner, A.E., Anderson, J.B., 2011. Cenozoic Glacial History of the Northern Antarctic Peninsula: A Micromorphological Investigation of Quartz Sand Grains. Tectonic, Clim. Cryospheric Evol. Antarct. Penins. 153–165.

Klostermann, L., Gischler, E., Storz, D., Hudson, J.H., 2014. Sedimentary record of late Holocene event beds in a mid-ocean atoll lagoon, Maldives, Indian Ocean: Potential for deposition by tsunamis. Mar. Geol. 348, 37–43. doi:10.1016/j.margeo.2013.11.014

Klostermann, L., Gischler, E., 2015. Holocene sedimentary evolution of a mid-ocean atoll lagoon, Maldives, Indian Ocean. Int. J. Earth Sci. 104(1), 289–307. doi:10.1007/s00531-014-1068-8

Kortekaas, S., 2002. Tsunamis, storms and earthquakes: distinguishing coastal flooding events. Ph.D. thesis, University of Coventry, 179 pp.

Kortekaas, S., Dawson, A.G., 2007. Distinguishing tsunami and storm deposits: An example from Martinhal, SW Portugal. Sediment. Geol. 200, 208–221. doi:10.1016/j.sedgeo.2007.01.004

Krinsley, D.H., Takahashi, T., 1962a. Surface textures of sand grains, an application of electron microscopy. Science 135, 923–925. doi:10.1126/science.135.3507.923

Krinsley, D.H., Takahaski, T., 1962b. Surface textures of sand grains–an application of electron microscopy: glaciation. Science 138, 1262–1264. doi:10.1126/science.138.3546.1262

Krinsley, D.H., Donahue, J., 1968. Environmental interpretation of sand grain surface textures by electron microscopy. Geol. Soc. Am. Bull. 79, 743–748. doi:10.1130/0016-7606(1968)79[743:EIOSGS]2.0.CO;2

Krinsley, D.H., Doornkamp, J.C., 1973. Atlas of quartz sand surface textures. Cambridge University Press, Cambridge. 91 pp.

Lane, P., Donnelly, J.P., Woodruff, J.D., Hawkes, A.D., 2011. A decadally-resolved paleohurricane record archived in the late Holocene sediments of a Florida sinkhole. Mar. Geol. 287, 14–30. doi:10.1016/j.margeo.2011.07.001

Lisá, L., 2004. Exoscopy of Moravian eolian sediments. Bull. Geosci. 79, 177–182.

Madhavaraju, J., Lee, Y.I., Armstrong-Altrin, J.S., Hussain, S.M., 2006. Microtextures on detrital quartz grains of upper Maastrichtian-Danian rocks of the Cauvery Basin, Southeastern India: implications for provenance and depositional environments. Geosci. J. 10, 23–34.

Mahaney, W.C., 2002. Atlas of sand grain surface, textures and applications. Oxford University Press, Oxford. 237 pp.

Mahaney, W.C., Dirszowsky, R.W., Milner, M.W., Menzies, J., Stewart, A., Kalm, V., Bezada, M., 2004. Quartz microtextures and microstructures owing to deformation of glaciolacustrine sediments in the northern Venezuelan Andes. J. Quat. Sci. 19, 23–33. doi:10.1002/jqs.818

Mahaney, W.C., Kalm, V., 2000. Comparative scanning electron microscopy study of oriented till blocks, glacial grains and Devonian sands in Estonia and Latvia. Boreas 29, 35–51. doi:10.1111/j.1502-3885.2000.tb01199.x

Mahaney, W.C., Dohm, J.M., 2011. The 2011 Japanese 9.0 magnitude earthquake: Test of a kinetic energy wave model using coastal configuration and offshore gradient of Earth and beyond. Sed. Geol. 239, 80–96. doi:10.1016/j.sedgeo.2011.06.001

Makvandi, S., Beaudoin, G., Mcclenaghan, B.M., Layton-Matthews, D., 2015. The surface texture and morphology of magnetite from the Izok Lake volcanogenic massive sulfide deposit and local glacial sediments, Nunavut, Canada: Application to mineral exploration. J. Geochemical Explor. 150, 84–103. doi:10.1016/j.gexplo.2014.12.013

Martins, L.R., 2003. Recent sediments and grain-size analysis. Gravel 1, 90–105.

Mauri, A., Davis, B.A.S., Collins, P.M., Kaplan, J.O., 2014. The influence of atmospheric circulation on the mid-Holocene climate of Europe: A data-model comparison. Clim. Past 10, 1925–1938. doi:10.5194/cp-10-1925-2014

McGranahan, G., Balk, D., Anderson, B., 2007. The rising tide: assessing the risks of climate change and human settlements in low elevation coastal zones. Environ. Urban. 19, 17–37. doi:10.1177/0956247807076960

Moral Cardona, J.P., Gutiérrez Mas, J.M., Sánchez, B. A., López-Aguayo, F., Caballero, M.A., 1997. Provenance of multicycle quartz arenites of Pliocene age at Arcos, southwestern Spain. Sediment. Geol. 112, 251–261. doi:10.1016/S0037-0738(97)00040-7

Morton, R.A., Gelfenbaum, G., Jaffe, B.E., 2007. Physical criteria for distinguishing sandy tsunami and storm deposits using modern examples. Sediment. Geol. 200, 184–207. doi:10.1016/j.sedgeo.2007.01.003

Mörner, N-A., 1996. Liquefaction and varve deformation as evidence of paleoseismic events and tsunamis. The autumn 10,430 BP case in Sweden. Quat. Sci. Rev. 15(8-9), 939–948. doi:10.1016/S0277-3791(96)00057-1

Mörner, N-A., 1999. Paleo-tsunamis in Sweden. Phys. Chem. Earth 24(5), 443–448. doi:10.1016/S1464-1909(99)00026-X

Mörner, N-A., 2008. Tsunami events within the Baltic. Polish Geol. Inst. Spec. Pap. 23, 71–76.

Muru, M., 2017. GIS-based palaeogeographical reconstructions of the Baltic Sea shores in Estonia and adjoining areas during the Stone Age. Diss. Geogr. Univ. Tartu. 64, University of Tartu Press, Tartu. 59 pp.

Mycielska-Dowgiałło, E., Woronko, B., 1998. Analiza obtoczenia i zmatowienia powierzchni ziarn kwarcowych frakcji piaszczystej i jej wartość interpretacyjna. Przegląd Geol. 46, 1275–1281.

Mycielska-Dowgiałło, E., Woronko, B., 2004. The degree of aeolization of Quaternary deposits in Poland as a tool for stratigraphic interpretation. Sediment. Geol. 168, 149–163. doi:10.1016/j.sedgeo.2003.12.006

Nartišs, M., Kalińska-Nartiša, E., 2017. An aeolian or a glaciolacustrine record? A case study from Mieļupite, Middle Gauja Lowland, northeast Latvia. Geologos 23, 15–28. doi:10.1515/logos-2017-0002

Newell, A.J., Kirby, G.A., Sorensen, J.P.R., Milodowski, A.E., 2015. The Cretaceous Continental Intercalaire in central Algeria: Subsurface evidence for a fluvial to aeolian transition and implications for the onset of aridity on the Saharan Platform. Palaeogeogr. Palaeoclimatol. Palaeoecol. 438, 146–159. doi:10.1016/j.palaeo.2015.07.023

Nielsen, P.R., Dahl, S.O., Jansen, H.L., 2016. Mid- to late Holocene aeolian activity recorded in a coastal dunefield and lacustrine sediments on Andøya, northern Norway. The Holocene 26(9), 1486-1501. doi: 10.1177/0959683616640050

Noren, A.J., Bierman, P.R., Steig, E.J., Lini, A., Southon, J., 2002. Millennial-scale storminess variability in the northeastern United States during the Holocene epoch. Nature 419, 821–824. doi:10.1038/nature01132

Nott, J.F., 2014. Palaeostorm Surges and Inundations, in: Ellis, J.T., Sherman, D.J. (Eds.), Coastal and Marine Hazards, Risks, and Disasters. Elsevier, pp. 129–152.

Orme, L.C., Davies, S.J., Duller, G.A.T., 2015. Reconstructed centennial variability of Late Holocene storminess from Cors Fochno, Wales, UK. J. Quat. Sci. 30, 478–488. doi:10.1002/jqs.2792

Otvos, E.G., 2011. Hurricane signatures and landforms-toward improved interpretations and global storm climate chronology. Sediment. Geol. 239, 10–22. doi:10.1016/j.sedgeo.2011.04.014

Peros, M., Gregory, B., Matos, F., Reinhardt, E., Desloges, J., 2015. Late-Holocene record of lagoon evolution, climate change, and hurricane activity from southeastern Cuba. The Holocene 25, 1483–1497. doi:10.1177/0959683615585844

Piotrowski, A., Szczuciński, W., Sydor, P., Kortys, B., Rzodkiewicz, M., Krzymińska, J., 2017. Sedimentary evidence of extreme storm surge or tsunami events in the southern Baltic Sea (Rogowo area, NW Poland). Geol. Q. 61(4), 973–986. doi:10.7306/gq.1385

Polovodova Asteman, I., Nordberg, K., Fipsson, H.L., 2013. The Little Ice Age: Evidence from a sediment record in Gullmar Fjord, Swedish west coast. Biogeosciences 10, 1275–1290. doi:10.5194/bg-10-1275-2013

Preusser, F., Muru, M., Rosentau, A., 2014. Comparing different post-IR IRSL approaches for the dating of Holocene coastal foredunes from Ruhnu Island, Estonia. Geochronometria 41, 342–351. doi:10.2478/s13386-013-0169-7

Qian, B., Saunders, M., 2003. Seasonal predictability of wintertime storminess over the North Atlantic 30, 2–6. doi:10.1029/2003GL017401

Quintela, M., Costa, P.J.M., Fatela, F., Drago, T., Hoska, N., Freitas, M.C., 2016. The AD 1755 tsunami deposits onshore and offshore of Algarve (south Portugal): Sediment transport interpretations based on the study of Foraminifera assemblages. Quat. Int. 408, 123–138. doi:10.1016/j.quaint.2015.12.029

Raukas, A., 2000. Investigation of impact spherules – a new promising method for the correlation of Quaternary deposits. Quat. Inter. 68-71, 241-252.

Refaat, A.A., Hamdan, M.A., 2015. Mineralogy and grain morphology of the aeolian dune sand of Toshka area , southeastern Western Desert , Egypt. Aeolian Res. 17, 243–254.

Renssen, H., Seppä, H., Crosta, X., Goosse, H., Roche, D.M., 2012. Global characterization of the Holocene Thermal Maximum. Quat. Sci. Rev. 48, 7–19. doi:10.1016/j.quascirev.2012.05.022

Rotnicki, K., Rotnicka, J., Goslar, T., Wawrzyniak-Wydorska, B., 2016. The first geological record of palaeotsunami on the southern coast of the Baltic Sea, Poland. Geol. Quat. 60(2), 417–440. doi:10.7306/gq.1294

Rutgersson, A., Jaagus, J., Schenk, F., Stendel, M., 2014. Observed changes and variability of atmospheric parameters in the Baltic Sea region during the last 200 years. Clim. Res. 61, 177–190. doi:10.3354/cr01244

Sabatier, P., Dezileau, L., Briqueu, L., Colin, C., Siani, G., 2010. Clay minerals and geochemistry record from northwest Mediterranean coastal lagoon sequence: Implications for paleostorm reconstruction. Sediment. Geol. 228, 205–217. doi:10.1016/j.sedgeo.2010.04.012

Sabatier, P., Dezileau, L., Colin, C., Briqueu, L., Bouchette, F., Martinez, P., Siani, G., Raynal, O., Von Grafenstein, U., 2012. 7000 years of paleostorm activity in the NW Mediterranean Sea in response to Holocene climate events. Quat. Res. 77, 1–11. doi:10.1016/j.yqres.2011.09.002

Seppä, H., Bjune, A.E., Telford, R.J., Birks, J.B., Veski, S., 2009. Last nine-thousand years of temperature variability in Norther Europe. Clim. Past 5, 523-535. doi: 10.5194/cp-5-523-2009

Skolasińska, K., Szczuciński, W., Mitręga, M., Jagodziński, R., Lorenc, S., 2014. Sedimentary records of 2010 and 2011 Warta River seasonal floods in the region of Poznań, Poland. Geol. Q. 58, 47-60. doi:10.7306/gq.1179

Soomere, T., Pindsoo, K., 2016. Spatial variability in the trends in extreme storm surges and weekly-scale high water levels in the eastern Baltic Sea. Cont. Shelf Res. 115, 53–64. doi:10.1016/j.csr.2015.12.016

Sorrel, P., Debret, M., Billeaud, I., Jaccard, S.L., McManus, J.F., Tessier, B., 2012. Persistent non-solar forcing of Holocene storm dynamics in coastal sedimentary archives. Nat. Geosci. 5, 1–5. doi:10.1038/ngeo1619Stanley, S., Deckker, P. De, 2002. A Holocene record of allochthonous, aeolian mineral grains in an Australian alpine lake; implications for the history of climate change in southeastern Australia. J. Paleolimnol. 27, 207–219. doi:10.1023/A:1014249404845

St. John, K., Passchier, S., Tantillo, B., Darby, D., Kearns, L., 2015. Microfeatures of modern sea-ice-rafted sediment and implications for paleo-sea-ice reconstructions. Ann. Glaciol. 56, 83–93. doi:10.3189/2015AoG69A586

Strotz, L.C., Mamo, B.L., Dominey-Howes, D., 2016. Effects of cyclone-generated disturbance on a tropical reef foraminifera assemblage. Sci. Rep. 6, 24–46. doi:10.1038/srep24846

Sweet, D.E., Soreghan, G.S., 2010. Application of Quartz Sand Microtextural Analysis to Infer Cold-Climate Weathering for the Equatorial Fountain Formation (Pennsylvanian-Permian, Colorado, U.S.A.). J. Sediment. Res. 80, 666–677. doi:10.2110/jsr.2010.061

Szkornik, K., Gehrels, W.R., Murray, A. S., 2008. Aeolian sand movement and relative sea-level rise in Ho Bugt, western Denmark, during the `Little Ice Age'. The Holocene 18, 951–965. doi:10.1177/0959683608091800

ter Braak, C.J.F., Šmilauer, P., 2012. Canoco Reference Manual and User's Guide: Software for Ordination (Version 5.0). Microcomputer Power. Ithaca, New York.

Tisdall, E.W., McCulloch, R.D., Sanderson, D.C.W., Simpson, I.A., Woodward, N.L., 2013. Living with sand: A record of landscape change and storminess during the Bronze and Iron Ages Orkney, Scotland. Quat. Int. 308–309, 205–215. doi:10.1016/j.quaint.2013.05.016

Toomey, M.R., Donnelly, J.P., Woodruff, J.D., 2013. Reconstructing mid-late Holocene cyclone variability in the Central Pacific using sedimentary records from Tahaa, French Polynesia. Quat. Sci. Rev. 77, 181–189. doi:10.1016/j.quascirev.2013.07.019

Tweel, A.W., Turner, R.E., 2012. Landscape-Scale Analysis of Wetland Sediment Deposition from Four Tropical Cyclone Events. PLoS One 7. doi:10.1371/journal.pone.0050528

Vaasma, T., 2008. Grain-size analysis of lacustrine sediments: A comparison of pre-treatment methods. Est. J. Ecol. 57, 231–243. doi:10.3176/eco.2008.4.01

Van den Biggelaar, D.F. a M., Kluiving, S.J., Balen, R.T. Van, Kasse, C., Troelstra, S.R., Prins, M.A., 2014. Storms in a lagoon: Flooding history during the last 1200 years derived from geological and historical archives of Schokland (Noordoostpolder, the Netherlands). Netherlands J. Geosci. 93, 175–196. doi:10.1017/njg.2014.14

Veski, S., Seppä, H., Ojala A.E.K., 2004. Cold event at 8200 yr. B.P. recorded in annually laminated lake sediments in eastern Europe. Geol. 32(8), 681–684. doi:10.1130/G20683.1

Veski, S., Heinsalu, A., Klassen, V., Kriiska, A., Lõugas, L., Poska, A., Saluäär, U., 2005. Early Holocene coastal settlements and palaeoenvironment on the shore of the Baltic Sea at Pärnu, southwestern Estonia. Quat. Inter. 130(1), 75–85. doi:10.1016/j.quaint.2004.04.033

Vilumaa, K., Tõnisson, H., Sugita, S., Buynevich, I.A., Kont, A., Muru, M., Preusser, F., Bjursäter, S., Vaasma, T., Vandel, E., Molodkov, A., Järvelill, J.I., 2016. Past extreme events recorded in the internal architecture of coastal formations in the Baltic Sea region. J. Coast. Research. SI 75, 775-779. doi:10.2112/SI75-156.1

Vitousek, S., Barnard, P.L., Fletcher, C.H., Frazer, N., Erikson, L., Storlazzi, C.D., 2017. Doubling of coastal flooding frequency within decades due to sea-level rise. Sci. Rep. 7, 1399. doi:10.1038/s41598-017-01362-7

Vos, K., Vandenberghe, N., Elsen, J., 2014. Surface textural analysis of quartz grains by scanning electron microscopy (SEM): From sample preparation to environmental interpretation. Earth-Science Rev. 128, 93–104. doi:10.1016/j.earscirev.2013.10.013

Wallace, D.J., Woodruff, J.D., Anderson, J.B., Donnelly, J.P., 2014. Palaeohurricane reconstructions from sedimentary archives along the Gulf of Mexico, Caribbean Sea and western North Atlantic Ocean margins. Sediment. Coast. Zo. from High to Low Latitudes Similarities Differ. 388, 481–501. doi:10.1144/SP388.12

Warrier, A.K., Pednekar, H., Mahesh, B.S.S., Mohan, R., Gazi, S., 2015. Sediment grain size and surface textural observations of quartz grains in late quaternary lacustrine sediments from

Schirmacher Oasis, East Antarctica: paleoenvironmental significance. Polar Sci. 10, 89–100. doi:10.1016/j.polar.2015.12.005

Wenthworth, C., 1922. A scale of grade and class terms for clastic sediments. J. Geol. 30(5), 377–392.

Woronko, B., Pisarska-Jamroży, M., 2016. Micro-Scale Frost Weathering of Sand-Sized Quartz Grains. Permafr. Periglac. Process. 27, 109–122. doi:10.1002/ppp.1855

Zelčs, V., Markots, A., Nartišs, M., Saks, T., 2011. Pleistocene Glaciations in Latvia, in: Ehlers, J., Gibbard, P.L., Hughes, P.D. (Eds.), Quaternary Glaciations - Extent and Chronology, Developments in Quaternary Science. Elsevier, Amsterdam, pp. 221–229. doi:10.1016/B978-0-444-53447-7.00018-0

Figures captions

Fig. 1. A - Location of the study area shown on the overview map (dashed lines show apparent uplift in mm yr^{-1} after Ekman, 1996). B – Surroundings of the Lake Lilaste with indication of the sampling site.

Fig. 2. Litology, mineral matter content and grain size of sediment from the Lilaste Lake.

Fig. 3. Bivariate plots. A – mean against standard deviation. B – standard deviation against skewness following the recommendation by Martins (2003) modified after Friedman (1967).

Fig. 4. Scanning electron micrographs of quartz grains from the Lilaste Lake: A – angular grain; B – subangular (=cracked) grain with bulbous edges (be) and big (>100 µm) conchoidal features (c); C – well-rounded grain with bulbous edges (be); C–D – mechanical microtextures, medium conchoidal features (c) and steps (s), overprinted chemical precipitation, F – surface with V-shaped percussion cracks (V), G – V-shaped percussion cracks (V) coupled with crescentic marks (cm); H – chemically-induced solution pits (p) and crevasses (cr); I – precipitation on grain surface; J – very intensively precipitated quartz grain; K – precipitation limited to depressions; L – oriented etch pits.

Fig. 5. Microtexture frequencies of the investigated quartz grains. LT and LI symbols refer to sample labels (*see* Fig.2 for details).

Fig. 6. Principal components analysis (PCA) of mineral matter (MinMatt), diatoms (Halophil, Marine/b, Freshwat), grain size (clay, silt, sand) and features of quartz grains (RM, EM/RM, EL, EM/EL, NU). PCA shows a variability among samples and represents major trends between environmental proxies. All sample loading is presented with given age of each sample.

Fig. 7. Results of the stratigraphically unconstrained CONISS cluster analysis of quartz grain surface features, diatom, mineral matter and grain size. Clusters are designated 1–6 on the left side of the diagram. X axis indicates percentages (%) and y axis shows samples organized in clusters according to CONISS cluster analysis.

Fig. 8. Stratigraphic diagram of quartz grain surface features: RM, EM/RM, EL, EM/EL (%); grain size: clay, silt and sand fractions (%). Columns of dots on the left side of the diagram show the stratigraphic distributions of samples falling into clusters defined by the stratigraphically unconstrained CONISS cluster analysis. Colour indicates each cluster: green – one; yellow – two; blue – three; red – four; orange – five; purple – six. Characteristics of each zone is described in Table 1. X axis represent % of each proxy, whereas y axis shows age, cal yr BP. On the right side marine and freshwater environment in Lilaste lake is indicated according to Grudzinska et al. (2017).

Table 1. Description of stratigraphically unconstrained cluster analysis results – clusters (zones).

Cluster (zone)	Description
1	Aqueous (EL) quartz grain domination (highest values) with almost no aeolian features (except a few EM/RM featured grains). Silt fraction values at 70% and sand from 20 to 30%. No fresh (NU) features on grains.
2	Highest values of sand, whilst lowest for silt fraction. Aeolian surface features observed sporadically, but aqueous particles still dominating (80–90%). Low clay abundance.
3	Lowest EL values, but highest for EM/EL. Few RM quartz grain features. Constant appearance of EM/RM features on grain surfaces.
4	NU (fresh) quartz grains appear only within this cluster. Nor RM, minor EM/RM presence.
5	Highest clay fraction abundance. Some RM and EM/RM quartz grains. Low to average (20–30%) EL grains, but high EM/EL (70%) grains. No NU features. Lowest values of sand.
6	Highest values of EM/RM and RM features on grains. Lowest EM/EL and low EL values except one peak reaching 55%. Average abundance of clay fractions. Low presence of sand (10–20%).

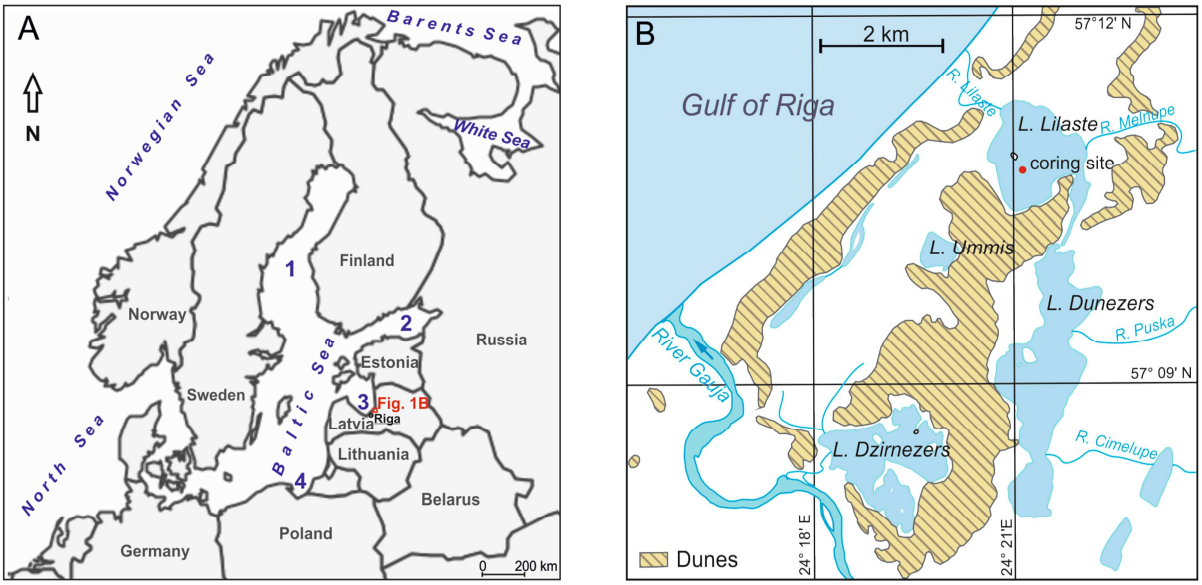

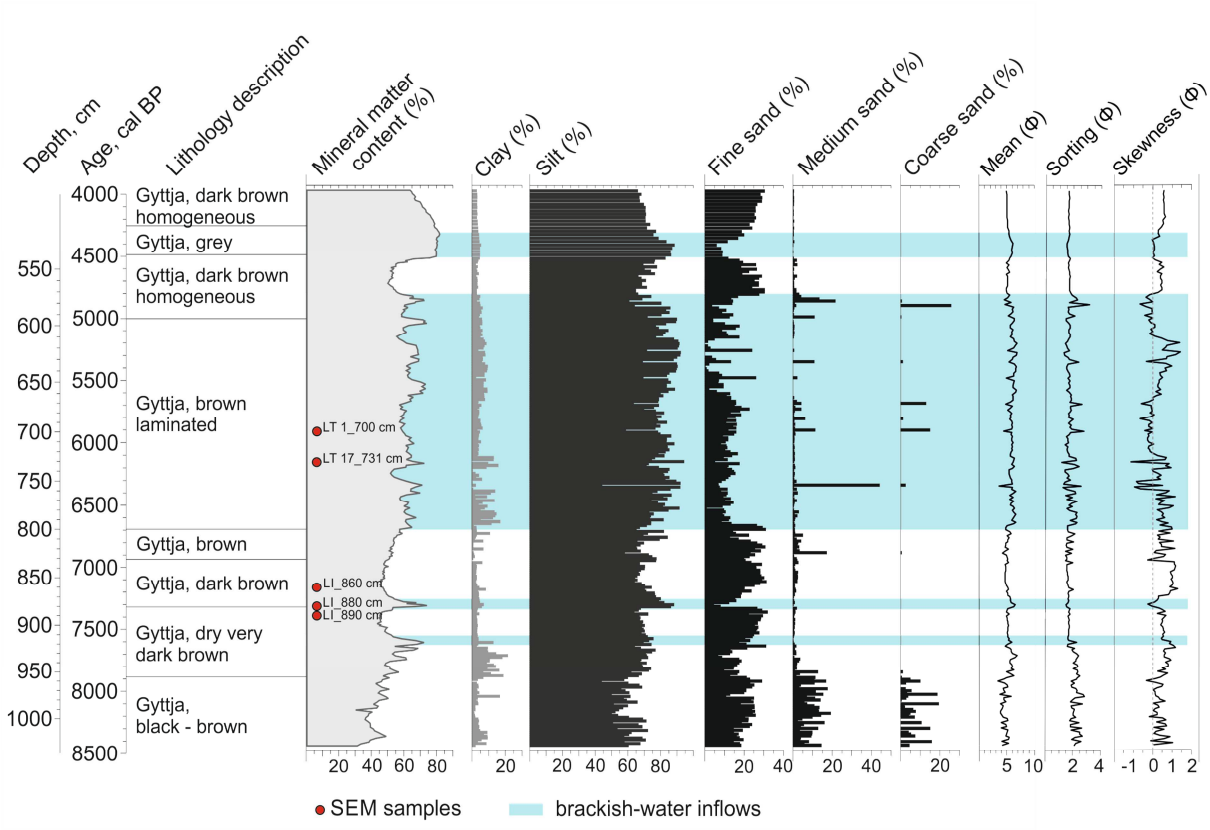

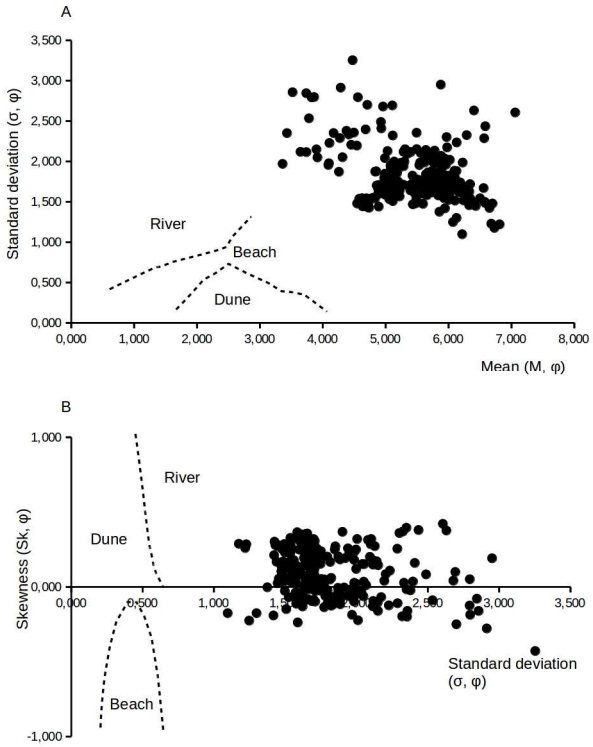

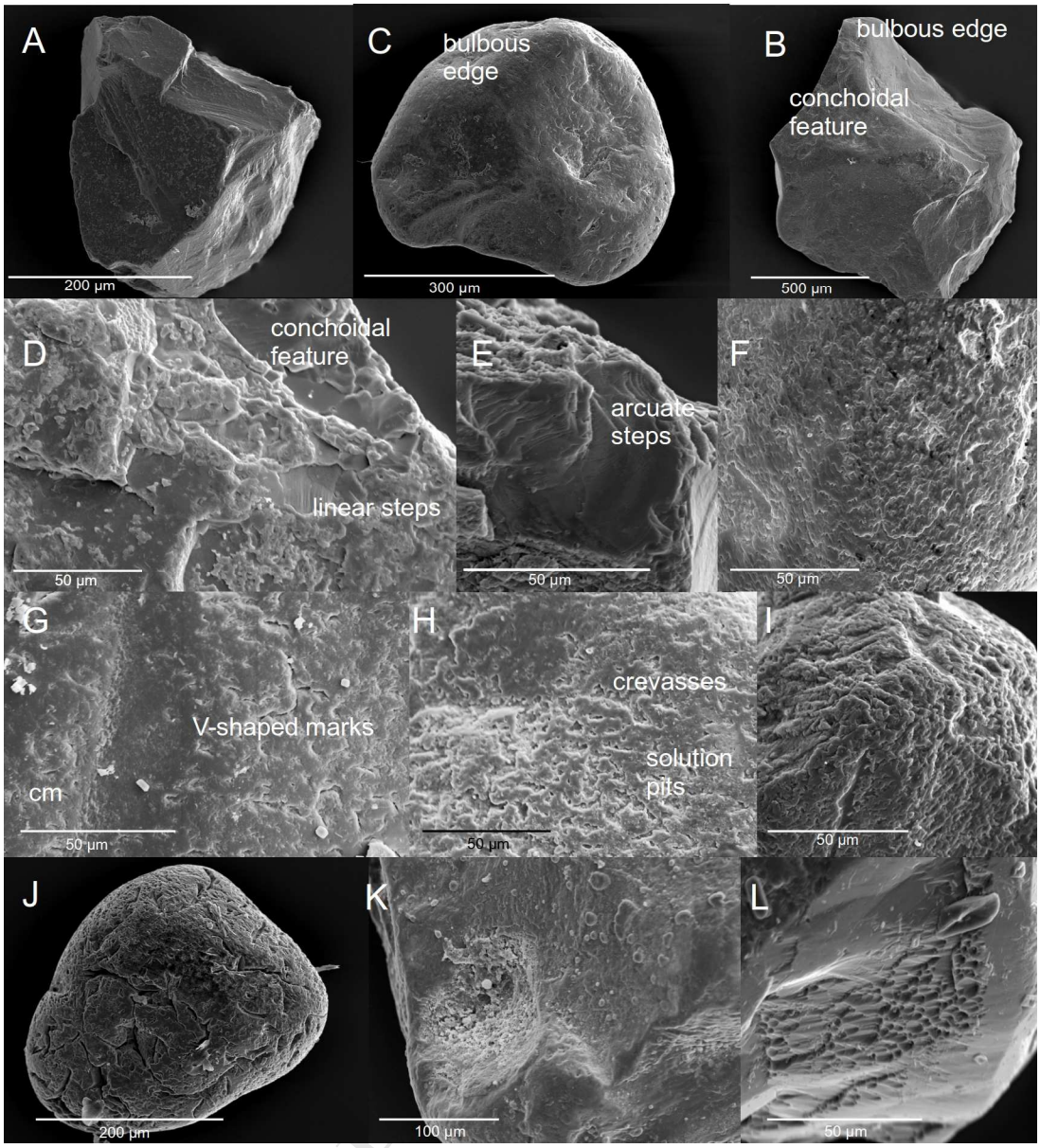

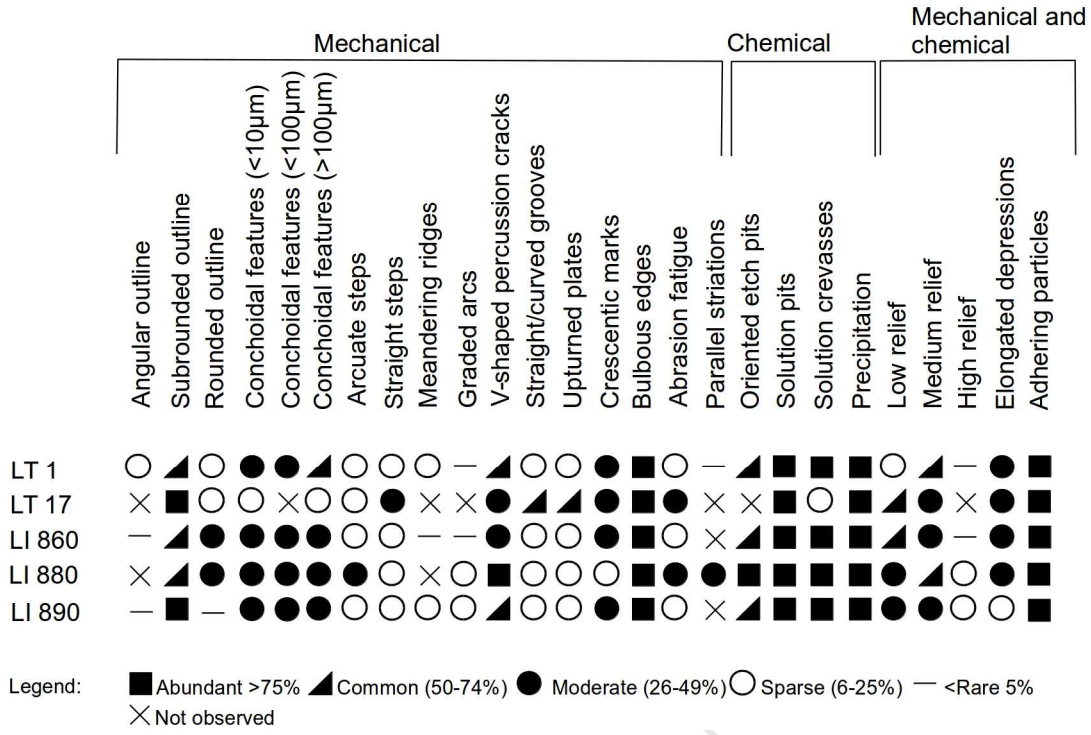

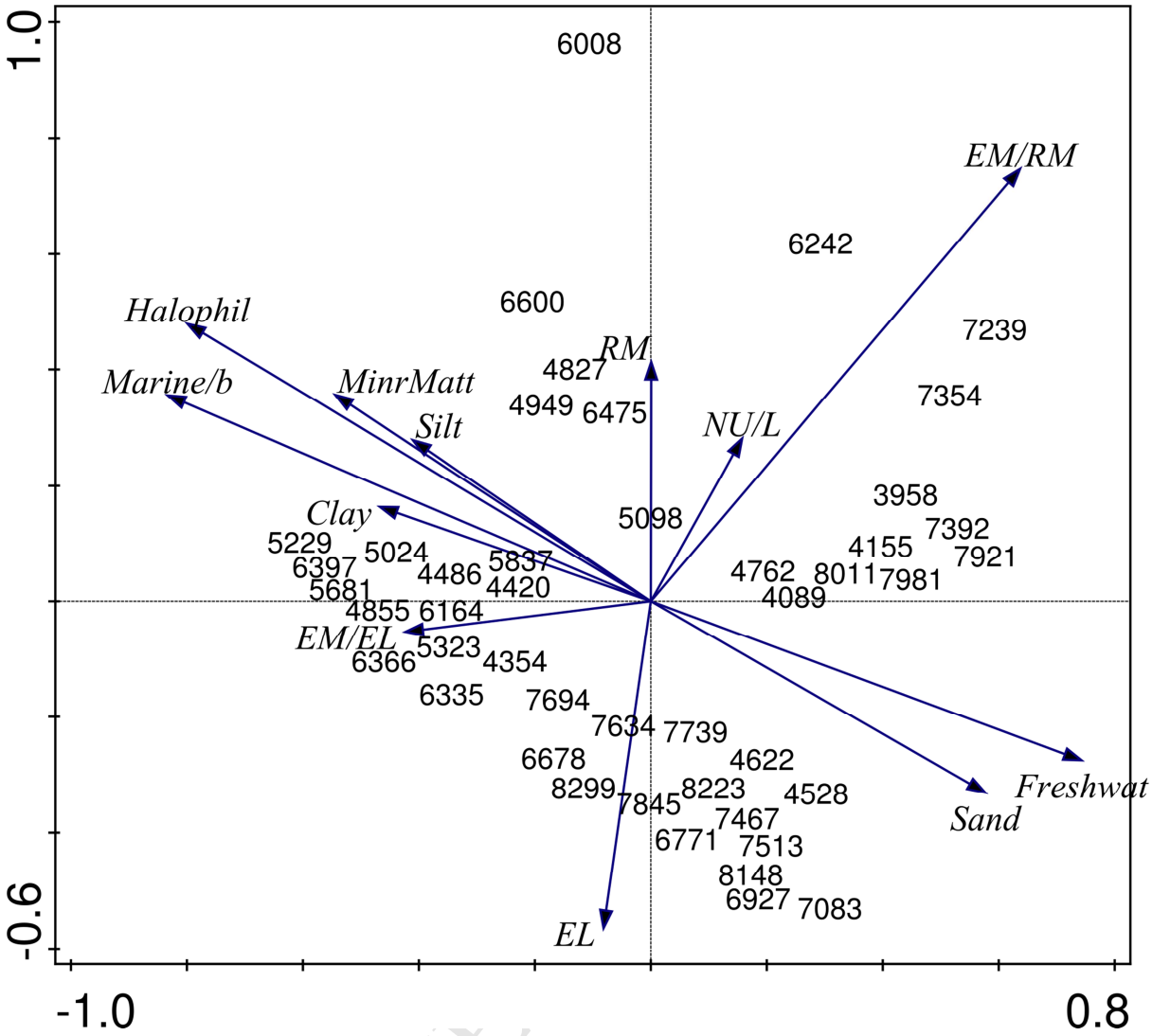
1.0
-0.6
-1.0
0.8
6008
EM/RM
6242
Halophil
6600
7239
RM
4827
Marine/b
MinrMatt
4949
6475
7354
Silt
NU/L
3958
Clay
5098
7392
5229
4155
7921
5024
5837
6397
4486
4420
4762
8011
7981
5681
4089
4855
6164
EM/EL
5323
6366
4354
6335
7694
7634
7739
6678
4622
Freshwat
8299
7845
8223
4528
Sand
7467
6771
7513
8148
6927
7083
EL

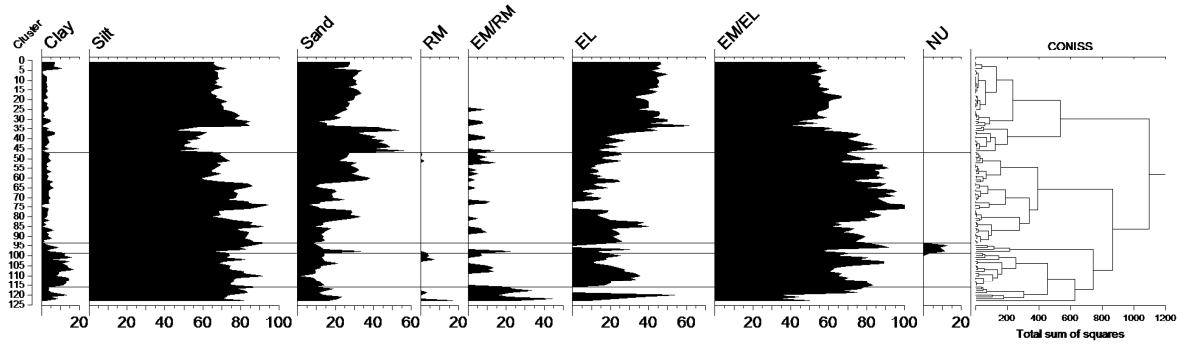

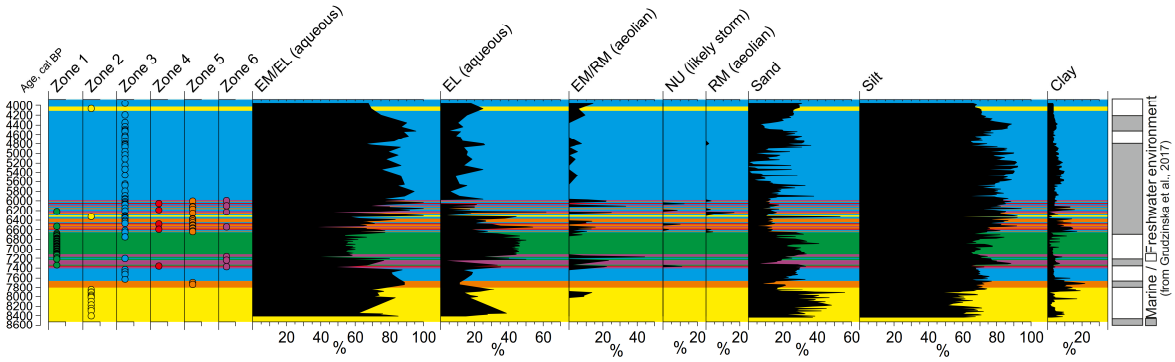

Highlights

Quartz grain characteristics combined with other proxies as indicators of depositional environments and past storminess

Three paleostorm events occurred at 7,300 cal yr BP, between 6,600 cal yr BP and 6,400 cal yr BP, and between 6,200 and 6,000 cal yr BP

Marine-terrestrial alternation occurred between 7,800 and 6,000 cal yr BP, and relatively stable marine conditions between 6,000 and 4,000 cal yr BP